frontiers in Chemical Biology

TYPE Original Research
PUBLISHED 21 May 2026
DOI 10.3389/fchbi.2026.1806456

OPEN ACCESS

EDITED BY
Mohammad Khursheed Siddiqi,
Virginia Commonwealth University,
United States

REVIEWED BY
Mohammad Amir,
Jamia Millia Islamia, India
Catherine Demery,
University of Michigan, United States

*CORRESPONDENCE
Giuseppe Floresta,
giuseppe.floresta@unict.it

RECEIVED 07 February 2026
REVISED 20 April 2026
ACCEPTED 21 April 2026
PUBLISHED 21 May 2026

CITATION
Floresta G, Patamia V, Granzotto A, Arillotta D, Papanti GD, Guirguis A, Corkery JM, Martinotti G, Sensi SL and Schifano F (2026) Tolazoline, an alpha-adrenergic antagonist, may also block xylazine at off-target sites as inferred from molecular docking.
Front. Chem. Biol. 5:1806456.
doi: 10.3389/fchbi.2026.1806456

Tolazoline, an alpha-adrenergic antagonist, may also block xylazine at off-target sites as inferred from molecular docking

Giuseppe Floresta[1,2]*, Vincenzo Patamia[2], Alberto Granzotto[3,4], Davide Arillotta[1,5], Gabriele Duccio Papanti[1,6], Amira Guirguis[7], John M. Corkery[1], Giovanni Martinotti[1,4], Stefano L. Sensi[3,4,8,9] and Fabrizio Schifano[1]

[1]Psychopharmacology, Drug Misuse and Novel Psychoactive Substances Research Unit, School of Life and Medical Sciences, University of Hertfordshire, Hatfield, United Kingdom, [2]School of Health, Medicine and Life Sciences, Department of Drug and Health Sciences, University of Catania, Catania, Italy, [3]Center for Advanced Studies and Technology – CAST, University G. d'Annunzio of Chieti-Pescara, Chieti, Italy, [4]Department of Neuroscience, Imaging, and Clinical Sciences, University G. d'Annunzio of Chieti-Pescara, Chieti, Italy, [5]Department of Neurosciences, Psychology, Drug Research, and Child Health, Section of Pharmacology and Toxicology, University of Florence, Florence, Italy, [6]Tolmezzo Community Mental Health Centre, ASUFC Mental Health and Addiction Department, Tolmezzo, Italy, [7]Swansea University Medical School, Swansea University, Swansea, United Kingdom, [8]Institute for Advanced Biomedical Technologies – ITAB, University G. d'Annunzio of Chieti-Pescara, Chieti, Italy, [9]Institute of Neurology, SS Annunziata University Hospital, University G. d'Annunzio of Chieti-Pescara, Chieti, Italy

Xylazine, a non-opioid α2-adrenoceptor agonist, is increasingly implicated in misuse and opioid-adulterated overdoses. Tolazoline, a non-selective α-adrenergic antagonist, is widely used in veterinary medicine to reverse xylazine-induced sedation and cardiovascular depression. Here, we combined molecular docking, molecular dynamics simulations, and *in silico* ADME (absorption, distribution, metabolism, and excretion)/Tox predictions to elucidate the pharmacological interplay between xylazine and tolazoline. Both compounds displayed comparable binding energies and stable interactions at the serotonin 5-HT_7 and κ-opioid receptors, supporting a competitive mechanism at shared receptor sites. Comparative *in silico* ADME profiling revealed that xylazine exhibits high blood–brain barrier penetration, extensive plasma protein binding, and rapid clearance, favouring potent but short-lived central nervous system effects. Conversely, tolazoline was predicted to demonstrate high lipo-solubility levels, low protein binding, large unbound fraction, and long half-life, enabling sustained peripheral α-blockade and sufficient central penetration to counteract xylazine's sedative and sympatholytic actions. These complementary pharmacokinetic and pharmacodynamic features suggest a mechanistic rationale for tolazoline's clinical efficacy as an antidote. By integrating receptor-level interactions with kinetic and distributional properties, our findings offer novel insights into the reversal of xylazine intoxication and generate testable predictions for transporter-mediated dynamics and PK/PD (Pharmacokinetic/Pharmacodynamic) modeling.

KEYWORDS
ADME, computational approaches, drug misuse, drug overdose, in silico studies, tolazoline, xylazine

1 Introduction

Over the last decade, the 'traditional' recreational drug scene has been supplemented - but not replaced - by the emergence of a range of novel psychoactive substances (NPS) (Schifano et al., 2015; Shafi et al., 2020) which are either newly created or existing drugs, including medications, now being used in novel ways (Schifano et al., 2017). Over the last few years, some veterinary, not-for-human, medications with α-2 adrenoceptor (α2-AR) agonist activities have entered the market as well (Papudesi et al., 2023; Pergolizzi et al., 2023). In particular, the α2-AR agonists xylazine and medetomidine have recently emerged as adulterants in the U.S. illicit drug supply, complicating public health monitoring and response. Indeed, Zhu et al. (2025) found that xylazine, whose injecting use is associated with skin ulcers and related infections, reports increased from just 2 in 1999 to 149 in 2015, then surged from 9,330 in 2021 to 25,047 in 2024, with the past 4 years accounting for more than 90% of all xylazine reports. Similarly, medetomidine, whose intake is frequently associated with hallucinations (Sibley et al., 2025), reports rose from 12 in 2021 to 2,276 in 2024. Whilst fentanyl was co-reported in 52.9% of xylazine reports (Zhu et al., 2025), xylazine has been reported as well in association with: stimulants (Kelly et al., 2025), alcohol, and benzodiazepines (Friedman et al., 2022; Dunn et al., 2024).

Although typically, xylazine is considered an unwanted adulterant (Hill et al., 2025), in a mixed-methods study, researchers found that about 1 in 4 (n = 13) of their interviewees used xylazine intentionally, presumably to experience the physical effects of the substance. A case of homicide involving fatal intoxication from xylazine overdose, without coadministration of other central nervous system drugs, was also described (Yu et al., 2025).

Xylazine alone is commonly referred to as "tranq"; conversely, when combined with opiates/opioids such as heroin or fentanyl, the mixture is usually termed "tranq dope" (Papudesi et al., 2023). Owusu-Antwi et al. (2025) carried out a 34-paper systematic review from 1957 to 2024 with a focus on xylazine misuse. They reported that this molecule intake was common among men aged 19–45 years, with dosages ranging from 40 to 4300 mg; no established toxic dosing, an antidote, or evidence-based treatment recommendations were identified.

Xylazine acute intoxication is potentially life-threatening, with the molecule acting as a central nervous system depressant and hence putatively potentiating the clinical effects of both opiates/opioids and remaining sedatives (Choi et al., 2023; Smith et al., 2023; Demery et al., 2025). Indeed, fatalities associated with the combination of fentanyl/xylazine have recently risen (Kariisa et al., 2023; Cano et al., 2024). In humans, overdoses associated with xylazine may resemble opioid overdoses, with its effects arguably not being reversed by naloxone (Choon et al., 2023). However, recent preclinical data found that naloxone precipitated withdrawal from both xylazine and fentanyl/xylazine co-administration (Bedard et al., 2024).

From a pharmacological perspective, xylazine activates both central and peripheral α2-adrenergic receptors (α2-ARs), resulting in muscle relaxation, reduced pain response, and depressed respiratory drive. The molecule may interact as well with serotonin 5-HT$_7$ (5-HT$_7$R (Floresta et al., 2025; Bedard et al., 2024); k-opioid (KOR); sigma 1 (σ1R); and sigma 2 receptors (Arena et al., 2018; Bedard et al., 2024), whilst typically considered a KOR agonist (Floresta et al., 2025; Bedard et al., 2024). To better understand xylazine action on opioid receptors, Smith et al. (2025) trained their experimental animals to discriminate the mu-opioid agonist, morphine, from saline; substitution tests were also carried out with fentanyl, xylazine, and their combinations. Whilst xylazine failed to substitute for morphine, its dose-dependently increased the duration of fentanyl's stimulus effects, which may partially explain its use in opioid misusers.

From the clinical pharmacokinetic point of view, xylazine bioavailability levels are poor with oral, nasal, rectal, and ocular exposure, with an elimination half-life of less than 1 h and rapid crossing of the blood–brain barrier (Garcia-Villar et al., 1981; Di Trana et al., 2024).

The management of xylazine and xylazine plus fentanyl intoxications and withdrawals may require a multidisciplinary approach, and is based on supportive care with airway management and hemodynamic stabilization, while alternative specific antagonists are under investigation (Rimawi and Hamlin, 2025). According to Kumar (2024) among a wide range of drugs investigated using a molecular docking approach (alpha-2 adrenergic receptor modulators, e.g., yohimbine, chlorpromazine, phentolamine, mianserine, spiperone, prazosin, alprenolol, propranolol, pindolol, atipamezole, dexmedetomidine, and tolazoline, and CNS stimulants, e.g., 4-aminopyridine, doxapram, and caffeine), prazosin emerged as a promising candidate capable of antagonizing xylazine. In animals, three reversal agents are currently available: atipamezole, yohimbine, and tolazoline. While atipamezole appears to be another promising agent, combined with naloxone (Mullins and Seger, 2025), the evidence for the effectiveness of yohimbine in humans is limited and inconclusive (Choi et al., 2024). In clinical and veterinary settings, tolazoline, a non-selective α-adrenergic antagonist, is widely employed as an effective antidote to reverse the sedative and cardiovascular effects of xylazine (Schifano et al., 2015). Although the pharmacological antagonism of xylazine by tolazoline is presumed to result from tolazoline binding to a-adrenergic receptors (Mohammad et al., 2024), it is not clear whether tolazoline exerts its action solely through blocking xylazine at a-adrenergic receptors or whether it directly competes with xylazine for occupancy at multiple receptor types. To be noted, tolazoline is generally well tolerated in animal use but it could be associated with transient tachycardia and mild hypertension, with potential ECG changes like QRS prolongation at high doses; gastrointestinal disturbances (e.g. diarrhea, increased motility), and mild neurological side effects such as restlessness and agitation may occur but are typically short-lived (Read et al., 2000). In the present study, the displacement mechanism of xylazine by tolazoline was investigated using a combination of molecular docking and molecular dynamics simulations.

2 Materials and methods

Marvin Sketch was used to create the 2D chemical structures, and the same software's MMFF94 force field was used to apply molecular mechanics energy minimization to each structure (Cheng

et al., 2000). The 3D geometry of all compounds was then optimized using the PM3 Hamiltonian (Stewart, 2004), as implemented in MOPAC 2016 package assuming a pH of 7.4. Using AutoDock's default docking parameters and a validated protocol, docking calculations were performed (Floresta et al., 2018; Floresta et al., 2019; Floresta et al., 2020; Fallica et al., 2021; Ielo et al., 2022; Patamia et al., 2023). The setup was done with YASARA (Krieger and Vriend, 2014). PDB id: 7XTC for 5-HT_7R and 4DJH for KOR were downloaded from the Protein Data Bank (www.rcsb.org) and used for calculations. The structures were downloaded from the Protein Data Bank and prepared with YASARA (25.5.19), specifically the structures were cleaned from all water molecules and the original ligands were removed. The studied binding pocket for the KOR was the conserved, solvent-exposed cavity located within the seven-transmembrane (TM) helical bundle on the cell exterior were the original ligand of 4DJH was located. The studied binding pocket for the 5-HT_7R was the serotonine binding pocket in the receptor where the original ligand of 7XTC was located. The MD simulations of the complexes were performed with the YASARA suite. A periodic simulation cell extending 10 Å from the protein surface was employed. A 15 Å cuboid cell was instead employed for the KOR. The cell was filled with water, with a maximum sum of all water bumps of 1.0 Å and a density of 0.997 g/mL. The setup included optimizing the hydrogen bonding network (Krieger et al., 2012) to increase the solute stability and a pK_a prediction to fine-tune the protonation states of protein residues at the chosen pH of 7.4 (Krieger et al., 2006). With an excess of either Na or Cl to neutralize the cell, NaCl ions were supplied at a physiological concentration of 0.9%. The simulation was run using the ff14SB force field for the solute, GAFF2, AM1BCC for ligands, and TIP3P for water. The cutoff was 10 Å for Van der Waals forces (the default used by AMBER) (Jakalian et al., 2002; Wang et al., 2004; Hornak et al., 2006; Maier et al., 2015), and no cutoff was applied to electrostatic forces. The equations of motions were integrated with multiple time steps of 2.5 fs for bonded interactions and 5.0 fs for nonbonded interactions at a temperature of 298 K and a pressure of 1 atm. Short MD simulation was run on the solvent only to remove clashes. The entire system was then energy minimized using a steepest descent minimization to remove conformational stress, followed by a simulated annealing minimization until convergence (<0.01 kcal/mol Å). Finally, 100 ns MD simulation without any restrictions was conducted, and the conformations were recorded every 250 ps. The MD trajectory, including the total potential energy of the system and the ligand movement RMSD were calculated with the YASARA *md_analyze* function. All molecular dynamics simulations performed in this study, including input files, trajectories, and analysis outputs, are publicly available in the Zenodo repository at: https://zenodo.org/records/19365577?token=eyJhbGciOiJIUzUxMiJ9.eyJpZCI6ImVkMzVlMjljLTdiMDYtNDZmNC1hYjc3LWY1ZmQ5NzhlZjA5MyIsImRhdGEiOnt9LCJyYW5kb20iOiIxYWU5ZTk2YWM1OWVkZWRiN2M1OTdlY2MzMDM1ZGY1MiJ9.5Jsu_VurEuiZHVPJWxunBFmHJgv3hX9NJYRSEWAm6TJQp-YbDfcG2guJnrYB2mMWq3Ue0YWb8EOiZzcSsO5d0A The repository includes complete datasets for both studied systems, as well as two additional files containing detailed post-simulation analyses (from YASARA *md_analyze* function). To facilitate data exploration, a structured list of all figures included in the analysis files is provided. Figure 1: A ray-traced picture of the simulated system. Figure 2: The solute oriented along the major axes. Figure 3: Simulation cell lengths as a function of simulation time. Figure 4: Total potential energy of the system as a function of simulation time. Figure 5: Potential energy components as a function of simulation time. Figure 6: Surface areas of the solute as a function of simulation time. Figure 7: Number of hydrogen bonds in the solute as a function of simulation time. Figure 8: Number of hydrogen bonds between solute and solvent as a function of simulation time. Figure 9: Protein secondary structure content as a function of simulation time. Figure 10: Per-residue protein secondary structure as a function of simulation time for each Res number. Figure 11: Per-residue number of contacts as a function of simulation time for each Res number. Figure 12: Radius of gyration of the solute as a function of simulation time. Figure 13: Solute RMSD from the reference structure as a function of simulation time. Figure 14: The Root Mean Square Fluctuation per solute protein/nucleic acid residue calculated from the average RMSF of the atoms constituting the residue. Figure 15: Visualization of the movement along PCA component 1 (to see the video look at the.mp4 file inside the respective folder). Figure 16: Visualization of the movement along PCA component 2 (to see the video look at the.mp4 file inside the respective folder). Figure 17: Visualization of the movement along PCA component 3 (to see the video look at the.mp4 file inside the respective folder). Figure 18: PCA eigenvalue as a function of PCA eigenvalue number. Figure 19: PCA components as a function of simulation time. Figure 20: PCA component as a function of PCA component 1. Figure 21: PCA component 3 as a function of PCA component 1. Figure 22: PCA component 3 as a function of PCA component 2. Figure 23-24: dynamic cross-correlation matrix. ADMETlab 3.0 was used for the ADMET prediction of the studied molecules using the *ADMET Evaluation* tools with the default parameters at the link: https://admetlab3.scbdd.com/(Fu et al., 2024) (the "Decision" column reported in ADMETlab 3.0 does not represent a direct measure of confidence in the predictions. Rather, it provides a qualitative, integrated assessment of the compound's overall drug-likeness based on multiple ADMET-related parameters).

3 Results

In silico studies were performed using AutoDockVina implemented in YASARA software. Using Marvin software, a study of the protonation stage of tolazoline at pH 7.4 was performed. To do this, docking studies within the serotonin 7 (5-HT_7) receptor pocket using both structures (PDB: 7XTC) were performed. SB-258719 was used as a reference ligand for the 5-HT_7 receptor in order to validate our method, yielding a calculated K_i of 20 nM (−10.5 kcal/mol) (Hagan et al., 2000), see Supplementary Figure S1. From Figure 1, which shows the 2D and 3D poses of tolazoline (1a and 1b) and protonated tolazoline (1c and 1d), it can be deduced how the protonation state affected the interaction of the ligand with the amino acid residues in the pocket. Tolazoline established a π-sulfur interaction with the Cys166 residue, to which are added numerous hydrophobic, alkyl, and carbon-hydrogen bond interactions with the Phe344, Val163, Ala247, Thr240, and Ser243 residues, respectively (Figures 1a,b).

10.3389/fchbi.2026.1806456

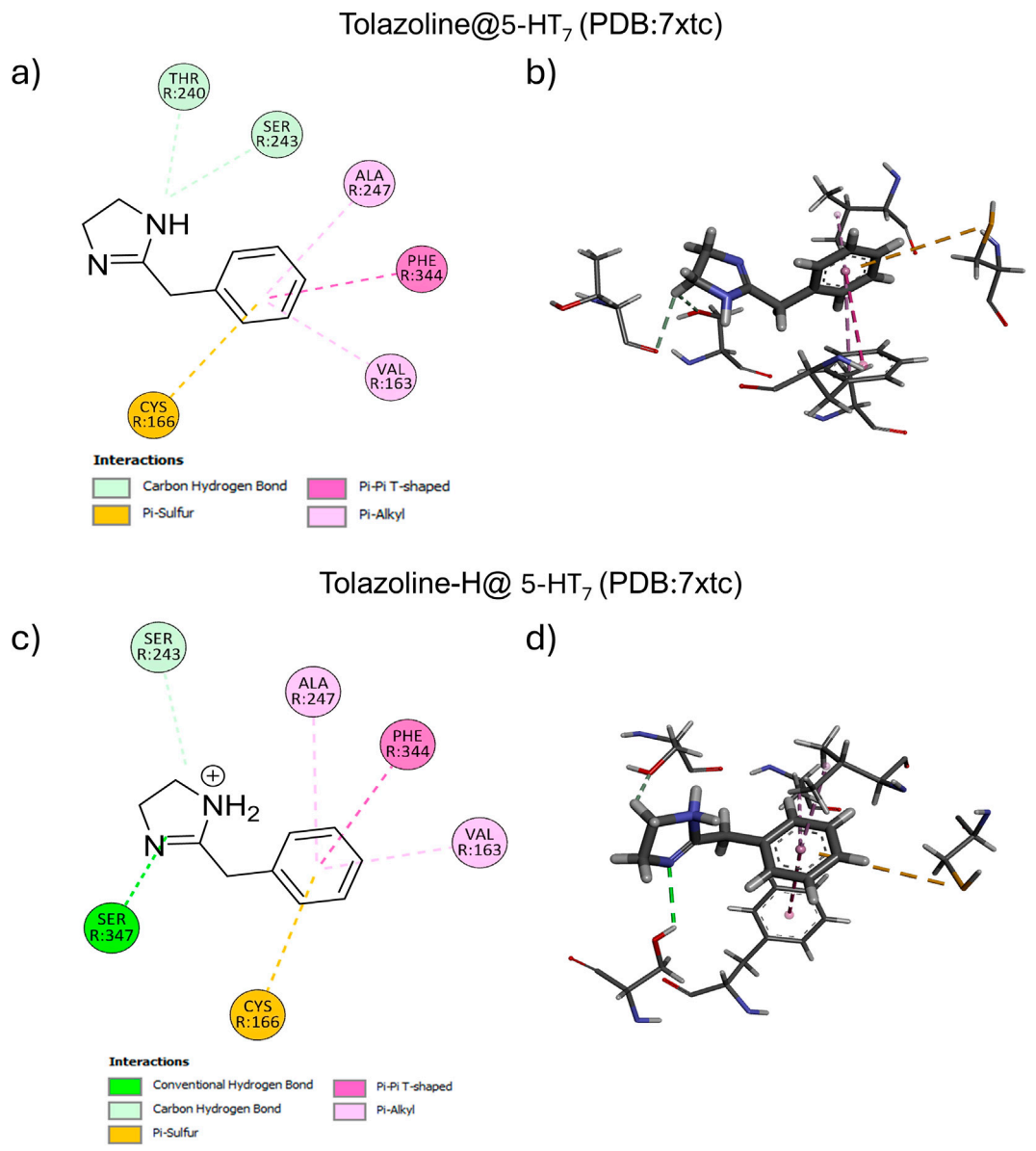

FIGURE 1
2D and 3D poses of tolazoline ((**a**) and (**b**)) and tolazoline-H ((**c**) and (**d**)) inside Serotonin 7 (5-HT$_7$) receptor.

Tolazoline-H was able to establish a hydrogen bond through nitrogen with the Ser347 residue; and, like unprotonated tolazoline, it retained the sulfur interaction with the Cys166 residue, the hydrophobic, alkyl, and carbon hydrogen bond interactions with the Phe344, Val163, Ala247, and Ser243 residues, respectively (Figures 1c,d). Despite the formation of a hydrogen bond, tolazoline-H had a slightly lower ΔG value than tolazoline and, consequently, also a lower binding energy, equal to 22.03 and 13.73 mM, respectively.

Comparing the poses with those of xylazine, either protonated or unprotonated, and within the same receptor, it was noted that the two drugs presented with residues and interactions in common, such as Phe344, Val163, and Cys166. Regarding the 5-HT$_7$ receptor (PDB: 7XTC), molecular docking analysis reported a binding energy of 6.80 kcal/mol for the protonated form of xylazine and 6.92 kcal/mol for its neutral species (Floresta et al., 2025). Differently, tolazoline, both protonated and unprotonated, interacted with other key residues such as Ser243, Ser347, Thr240, and Ala247.

To further study the tolazoline@7xtc complex, a 100 ns molecular dynamics (MD) simulation was conducted. Considering that there was minimal difference in predicted interactions between protonated and non-protonated structures, the dynamics were conducted on the non-protonated structure.

Analysis of the total energy graph of tolazoline@7xtc revealed that the complex immediately reached equilibrium and remained stable throughout the duration of the dynamics (Figure 2a). This was confirmed by the RMSD (root mean square deviation) graph of the complex (Figure 2b), which showed three fluctuations: one initially at 40 ns, followed by a second at 60 ns, and the last at 80 ns.

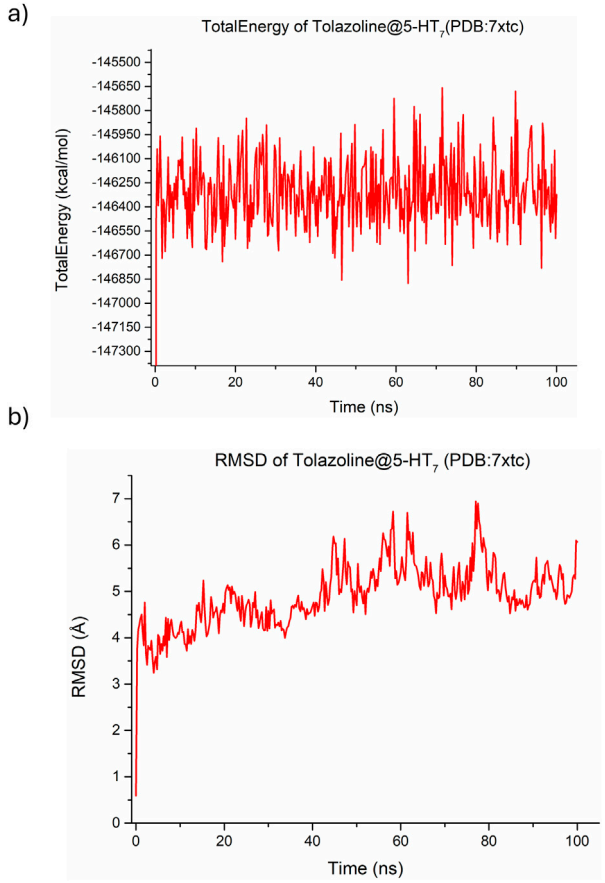

FIGURE 2
Total energy **(a)** and RMSD **(b)** for tolazine@7xtc complex.

Nevertheless, thanks to the dense network of interactions, as was the case with xylazine, the complex remained constantly within the binding site throughout the simulation.

U69,593 was used as a reference ligand for the KOR receptor in order to validate our method, yielding a calculated K_i of 54 nM (−9.92 kcal/mol) (Costanzo et al., 2023), see Supplementary Figure S1.

Similarly, both the protonated and unprotonated forms of tolazoline were also used for docking studies with human KOR (PDB: 4DJH). Figures 3a,b show the 2D and 3D poses of unprotonated tolazoline, respectively, where it was seen that it formed carbon-hydrogen bonds with residues Thr111 and Gln115 and π-sigma interaction with Tyr320, π-π stacked interaction with Trp287, and π-alkyl interactions with residues, Ile290 and Ile316. The 2D and 3D poses of the protonated form are shown in Figures 3c,d, respectively. In this case, the presence of the proton allows tolazoline-H to form a salt bridge with the Asp138 residue and a hydrogen bond with Thr111. Added to these are the carbon-hydrogen bonds with the Gln115 and Tyr320 residues and the stacked π-p and T-shaped interactions with Trp287 and π-alkyl interactions with residues Ile316 and Ile290. Despite the two electrostatic interactions, the salt bridge and the hydrogen bond, tolazoline and tolazoline-H presented with similar binding energies, 16.53 and 16.81 mM, respectively. Comparing the poses of unprotonated tolazoline with those of unprotonated xylazine within the k-opioid receptor, it was seen that 5 out of 6 residues were in common. In some cases, the type of interaction was also common, as for residues Gln115, Ile290 and Ile315. For the KOR receptor (PDB: 4DJH), the binding energies for xylazine were calculated at 6.49 kcal/mol for the protonated state and 7.10 kcal/mol for the unprotonated form (Floresta et al., 2025). The protonated structures of xylazine and tolazoline showed unique residues and interactions in common compared to the unprotonated molecules, such as Asp138, Trp287, Ile290 and Ile316. In both structures, protonated and non-protonated, tolazoline interacted with one more residue than xylazine, namely Thr111.

The tolazoline@4djh complex was also studied using the 100 ns molecular dynamics, again on the unprotonated structure. From the analysis of the images showing the total energy of the complex (Figure 4a), it was seen how the interactions kept tolazoline firmly inside the receptor. This was also confirmed by the RMSD of the complex (Figure 4b), where, after a small fluctuation at 10 ns, the complex showed no instability for the rest of the dynamics, unlike the complex with xylazine, where fluctuations were already evident in the first 50 ns.

Considering the predicted energy involved in the interaction at the molecular level between the two molecules was very similar, a detailed comparison was made of their *in silico* ADME (Absorption, Distribution, Metabolism, Excretion) and toxicity profiles.

3.1 Absorption

Drug absorption is influenced by a delicate interplay of solubility, membrane permeability, intestinal transport, and first-pass metabolism (Azman et al., 2022). Both tolazoline and xylazine are relatively small molecules (MW 160.1 vs. 220.1 Da), which places them in a favourable size range for passive diffusion. However, they differ significantly in lipophilicity, solubility (tolazoline: logS = −1.64, logP = 1.11, logD = 0.23; xylazine: logS = −3.01, logP = 2.14, logD = 2.19), and predicted permeability outcomes. Tolazoline is predicted to possess higher levels of aqueous solubility (logS closer to 0) and significantly lower lipophilicity (logP ~1). This physico-chemical profile may suggest that tolazoline may be readily dissolved in gastrointestinal fluids, favouring absorption under aqueous conditions, but less prone to strong partitioning into lipid membranes. By contrast, xylazine is more lipophilic and less soluble, which may limit dissolution in the gastrointestinal tract whilst facilitating passive membrane diffusion once in solution.

Both compounds are strongly predicted as P-glycoprotein (P-gp) substrates (tolazoline 0.93; xylazine 0.94). This implies that intestinal efflux transport may significantly restrict net oral absorption, especially at therapeutic doses (Kwon et al., 2004). Neither compound is predicted to be a strong P-gp inhibitor, minimizing the likelihood of transporter-based drug–drug interactions from the inhibitory side.

Both compounds are predicted to have poor oral absorption based on their pharmacokinetic profiles. Specifically, Human Intestinal Absorption (HIA)—which represents the probability of a drug crossing the intestinal barrier—is estimated at 0.002 for tolazoline and 0.0 for xylazine. Furthermore, the values for oral bioavailability (F), which indicate the fraction of the dose that reaches systemic circulation, are extremely low at both the 20% (F20%) and 50% (F50%) probability thresholds (tolazoline:

10.3389/fchbi.2026.1806456

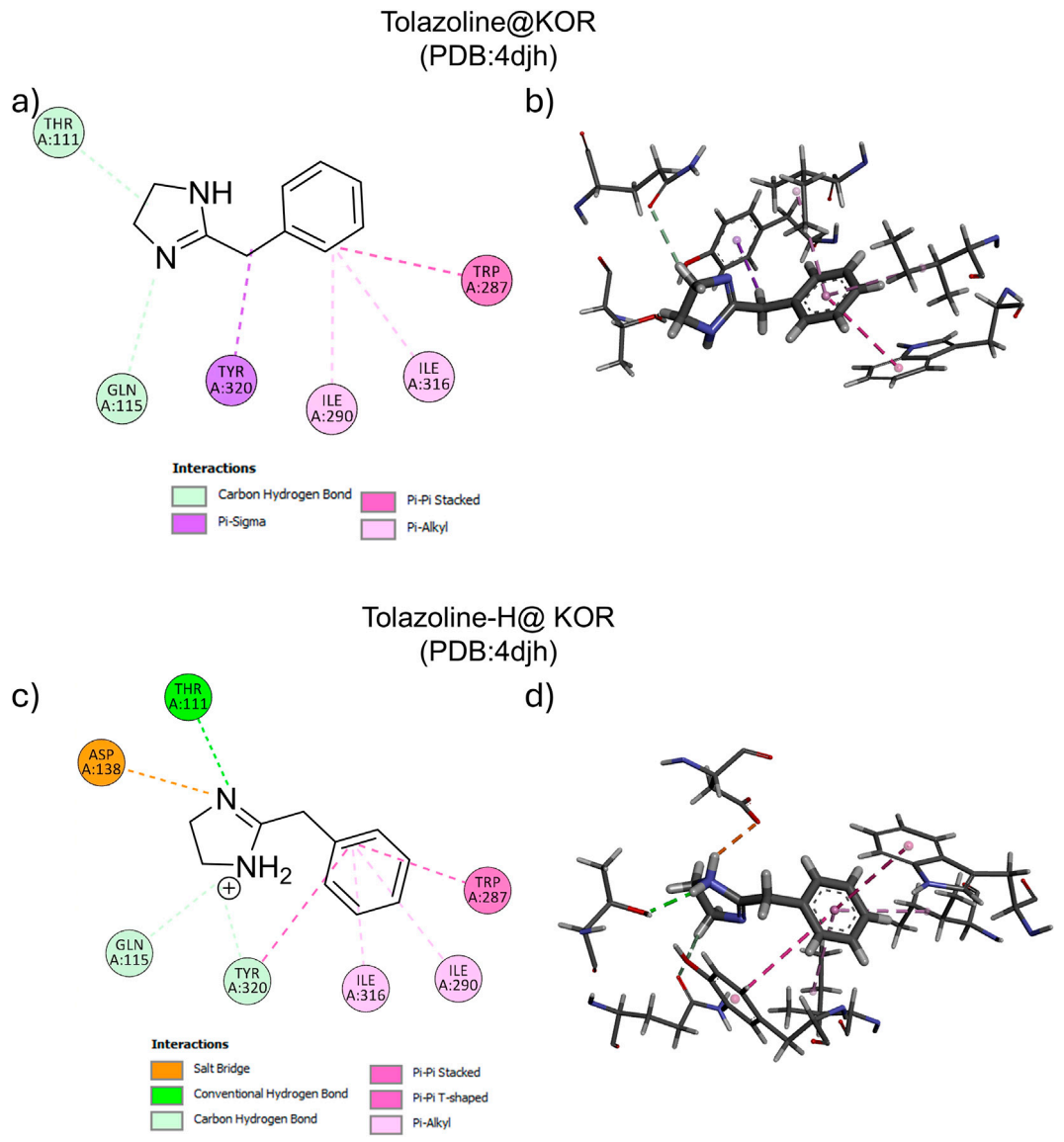

FIGURE 3
2D and 3D poses of tolazoline (**(a)** and **(b)**) and tolazoline-H (**(c)** and **(d)**) inside the k-opioid receptor.

F20% = 0.025, F50% = 0.075; xylazine: F20% = 0.0, F50% = 0.007). Hence, both are unlikely to achieve robust systemic exposure via the oral route, with xylazine being predicted to be slightly worse. This is consistent with its clinical use primarily by parenteral routes in veterinary medicine (Santonastaso et al., 2014). Tolazoline, however, has historically been used orally in humans, suggesting that while predictions indicate limited absorption, *in vivo* absorption is not negligible, perhaps due to formulation strategies or transporter involvement that are not fully captured in our *in silico* models.

3.2 Distribution

The plasma protein binding and free fraction for the two molecules are predicted to be completely different, with tolazoline having a PPB ~25% and a fraction unbound of (Fu) ~68%, whereas xylazine may present with a PPB ~94% and a Fu ~4%. As a result, one could argue that tolazoline circulates largely in unbound form, enabling wide tissue distribution and free access to pharmacological targets. Conversely, xylazine is highly protein-bound, which reduces free drug concentrations whilst delaying tissue retention, potentially contributing to its strong and sustained sedative effects. Considering the volume of distribution (VDss, tolazoline: 0.48 L/kg; xylazine: 0.33 L/kg), both fall within the moderate distribution range, with tolazoline being predicted to distribute slightly more extensively into tissues relative to plasma, consistent with its higher unbound fraction. From the blood–brain barrier (BBB) penetration perspective, a relevant difference is predicted between the two molecules presented with a relevant difference (e.g., tolazoline: BBB probability 0.27 (low likelihood); xylazine: BBB probability 0.99 (very high likelihood)). Xylazine is predicted to cross the BBB efficiently, aligning with its potent central

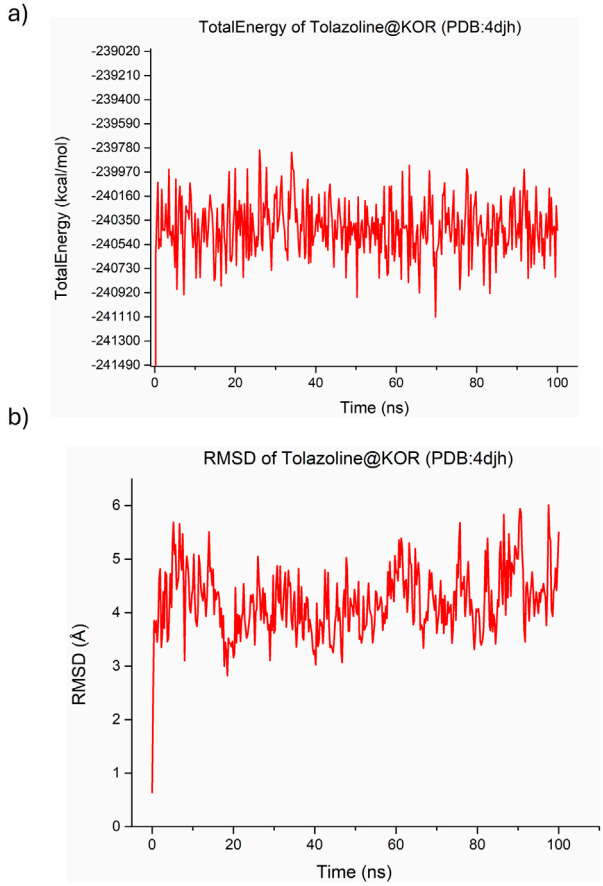

FIGURE 4
Total energy **(a)** and RMSD **(b)** for tolazine@k-opioid complex.

sedative and analgesic properties. Conversely, tolazoline, with its poor predicted BBB penetration, exerts effects largely in the peripheral vasculature, consistent with its clinical role as a vasodilator and α-adrenergic antagonist without strong central nervous system actions (Stoeckelhuber et al., 2003). Finally, although both interact with hepatic transporters, *in silico* data suggest that tolazoline appears to be more involved in inhibiting absorption, whilst xylazine appears to interfere more with efflux pumps.

3.3 Metabolism

Both compounds are predicted to be extensively metabolized by cytochrome P450 enzymes, although with markedly different interaction profiles (see Supplementary material). Thus, tolazoline appears more metabolically stable, is cleared more slowly, and is prone to interactions with CYP2D6 metabolism, both as a substrate and a strong inhibitor. This may suggest potential drug–drug interaction liabilities in humans, especially with medications metabolized by CYP2D6 (Nahid and Johnson, 2022). Conversely, xylazine shows broad substrate promiscuity, being metabolized by essentially all major drug-metabolizing CYPs. However, it is predicted to be metabolically unstable, consistent with its rapid clearance and short half-life (0.89 h).

3.4 Toxicity

Tolazoline is a non-selective α-adrenergic antagonist, hence vasodilation, reflex tachycardia, and hypotension can be observed. Conversely, in xylazine (α_2-agonist) intoxication, bradycardia, AV block, and hypotension can be identified. Xylazine shows substantially greater predicted hepatotoxic potential, consistent with reports of liver injury in animals and humans exposed chronically (Iacopetta et al., 2025; Yi et al., 2025). Both compounds raise concerns about genotoxicity, with tolazoline skewing toward carcinogenicity risk and xylazine toward mutagenicity. Respiratory toxicity is high for both, but tolazoline exhibits a greater neurotoxic liability, whereas xylazine is more ototoxic.

4 Discussion

To our knowledge, this is the first study to compare the potential drug-drug interaction between xylazine and tolazoline using a combination of molecular docking techniques, molecular dynamics simulations and *in silico* ADME/Tox predictions. Current findings have shown, through molecular dynamics studies, that tolazoline and xylazine exhibit comparable binding energies and stable interactions with KOR and 5-HT_7 receptors, suggesting that their affinities for these sites are of a similar magnitude. This may provide a plausible molecular explanation for the clinical efficacy of tolazoline as an antidote; indeed, by occupying receptor binding sites with similar stability, tolazoline may effectively prevent or reduce xylazine's ability to show pharmacological effects.

Building upon the molecular docking and dynamics results, which revealed comparable predicted binding energies and interaction stability for xylazine and tolazoline at their receptor sites, we extended our investigation to the pharmacokinetic dimension. Since similar binding affinities alone cannot fully account for the clinical efficacy of tolazoline as an antidote, it became essential to evaluate how ADME properties may influence the net pharmacological outcome. By integrating molecular-level receptor interactions with *in silico* ADME predictions, we aimed to provide a comprehensive explanation of how tolazoline could displace xylazine from 5-HT_7 and KOR receptors.

Xylazine is predicted by its ADME profile to achieve rapid, high-level, CNS exposure, due to very high BBB penetration probability; high lipophilicity relative to tolazoline; and very low free fraction that nonetheless may be enough to occupy high-affinity α2-adrenoceptors. These data may explain xylazine-related sedation, analgesia, and muscle relaxation. Tolazoline, in contrast, presents as a moderately lipophilic, highly unbound, short-to-intermediate half-life molecule; overall, this may favor fast receptor access in plasma and tissues, limited but not negligible CNS penetration, and sustained target coverage over the timeframe in which xylazine is being cleared. When co-administered after xylazine, both tolazoline pharmacokinetics (e.g., high fraction unbound, longer t½) and transporter profile (e.g., shared P-gp substrate status) may enable sufficient CNS exposure to competitively antagonize α2-adrenoceptors and robust peripheral α-blockade to restore

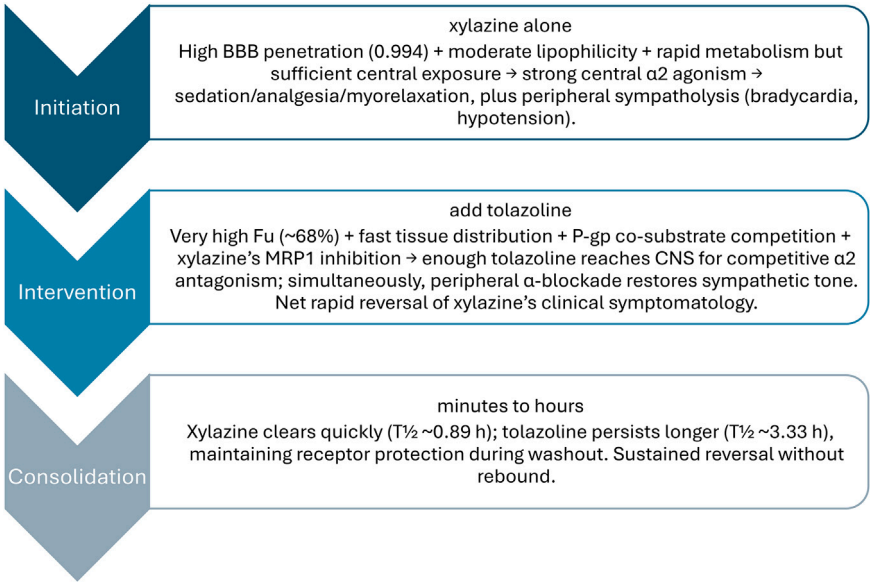

FIGURE 5
Proposed ADME-based pharmacokinetic (PK) paradigm derived from *in silico* simulations. This schematic representation illustrates the hypothetical ADME behavior of the studied compounds, based exclusively on computational predictions and not on experimentally measured pharmacokinetic data. Abbreviations: Fu, fraction unbound in plasma; MRP1, multidrug resistance-associated protein 1; BBB, blood–brain barrier; P-gp, P-glycoprotein.

sympathetic tone; taken together, these data may be consistent with a clinically effective "antidote-like" reversal of tolazoline over xylazine.

Xylazine is strongly predicted to penetrate the BBB, with a probability level of 0.994; low fraction unbound in plasma (Fu ≈ 4.26%); and high plasma protein binding (PPB ≈94.3%). Although Fu levels are low, the compound distribution characteristics (VDss ≈0.33 L/kg) and high lipophilicity (logP ≈2.14; logD ≈2.19) levels favor CNS access. Overall, this profile is consistent with a drug that rapidly occupies central receptors to produce sedation, analgesia, and muscle relaxation. Conversely, tolazoline is predicted to possess modest BBB penetration (e.g., BBB probability ≈0.271); substantially high levels of unbound fraction (Fu ≈ 67.7%); low PPB (≈25.5%); and low lipophilicity (logP ≈1.11; logD ≈0.23) levels. These data are consistent with the assumption that tolazoline circulates largely free, reaches a rapid equilibrium with extracellular sites, and rapidly reaches the related receptors, with its membrane permeability being permissive.

The CNS exposure gap is largely predicted to be in xylazine's favor at baseline; however, tolazoline starts with a key kinetic advantage, i.e., a very large unbound pool that can drive rapid target engagement where access is feasible. Even if its absolute brain penetration is low, the unbound concentration available to enter the CNS immediately after dosing is high, and a portion of this pool will cross the BBB, particularly so if transporter dynamics at the BBB level are transiently favourable. Once a small but sufficient CNS concentration is achieved, competitive antagonism can rapidly decrease xylazine's effects, whilst peripheral α-blockade restores sympathetic outflow and hence counteracts the xylazine-related bradycardia and hypotension. Together, these central and peripheral actions align with what one would expect from the ADME contrast.

Xylazine is predicted to be HLM-unstable (Human Liver Microsomes) (i.e., instability probability ≈0.992), with moderate plasma clearance of approximately 10.9 mL/min/kg and an ultra-short half-life (i.e., T½ ≈ 0.89 h), all of which are consistent with a relatively rapid systemic washout.

Tolazoline is predicted to be HLM-stable (e.g., instability probability ≈ 0.031), with borderline-high clearance (≈15.0 mL/min/kg) and a longer half-life (T½ ≈ 3.33 h), providing a several-fold longer coverage window than xylazine. The *in silico* predictions are in good agreement with experimentally measured pharmacokinetic parameters. Xylazine is known to undergo rapid clearance, with reported half-life values in the range of 23–50 min, while tolazoline exhibits a significantly longer half-life (Casbeer and Knych, 2013; Hoffman et al., 2024). The ability of the model to reproduce this marked difference in metabolic stability between the two compounds supports its predictive validity. In a reversal scenario, the antagonist that outlasts the agonist has an inherent temporal advantage. Indeed, tolazoline's longer T½ ensures that once it reaches relevant effect compartments, its antagonism persists, whilst xylazine concentrations are falling quickly. This kinetic "cross-over" (e.g., antagonist persists; agonist fades) is a central design principle in antidote pharmacology and is clearly reflected in the predicted T½ gap.

Both xylazine and tolazoline are predicted P-gp substrates, with high probability levels (e.g., ≈0.939 and ≈0.925, respectively). Neither is predicted to be a P-gp inhibitor. Xylazine is also predicted to be a potent MRP1 inhibitor, with a probability ≈ of 0.994, whereas tolazoline is near the decision boundary for MRP1 inhibition, at ≈ 0.496. Neither compound is predicted to inhibit BCRP (Breast Cancer Resistance Protein). Shared P-gp substrate status means tolazoline can compete with xylazine for efflux capacity at the BBB. Xylazine's MRP1 (Multidrug Resistance-associated Protein 1) inhibition may additionally alter BBB efflux

tone for co-administered cations, potentially reducing parallel efflux routes and further nudging tolazoline brain exposure upward, at least transiently. Although this is an inference, since the reports provided are inhibitor/substrate probabilities as opposed to quantitative Ki's, are the directionality is clear, e.g., xylazine tends to inhibit an efflux pump (MRP1) that might otherwise remove cationic species; tolazoline sits near the boundary (≈0.496) and is very highly unbound, so any efflux constraint loosened by xylazine could favor tolazoline retention in the brain interstitium. The combination of these factors, e.g., competition for P-gp and xylazine-driven MRP1 inhibition, offers an ADME-grounded rationale for how tolazoline gains sufficient levels of central access, and rapidly enough, to produce a clinically meaningful reversal even though its stand-alone BBB probability is low.

Both compounds are predicted to have very poor oral HIA (xylazine HIA probability of being "HIA+" = 0.0; tolazoline ≈0.002) and low oral F-flags (F20–F50%, flagged as negative probabilities for both). These de-emphasize the role of oral dosing in acute settings and reinforce tolazoline IV use for reversal of xylazine effects. In the context of an acute reversal, the key question is not total exposure, but time to receptor occupancy. Tolazoline's very high Fu means that after IV dosing, the entire circulating pool is largely available to distribute and bind, whilst being limited mainly by perfusion and permeability and not by protein binding equilibria.

A substantial metabolic overlap exists between the two molecules. Both xylazine and tolazoline are predicted substrates of CYP1A2 and CYP2D6, with xylazine additionally flagged as a CYP2C19 and CYP3A4 substrate (all ≈1.0 probabilities). Tolazoline is predicted to be a potent CYP2D6 inhibitor (probability = 1.0) and a CYP3A4 substrate (≈0.995), whilst xylazine shows a CYP2D6 inhibitor probability ≈ of 0.764 and a clear CYP3A4 substrate status. Whilst tolazoline's 2D6 inhibition could, in principle, slow xylazine metabolism, that would not explain the rapid clinical reversal and is, if anything, a counteracting pharmacodynamic-independent effect.

Taken together, all PK parameters describe a kinetic and distributional environment that strongly favors reversal of tolazoline over xylazine, as described in Figure 5. Because tolazoline is highly unbound (≈68% Fu) and distributes quickly to well-perfused peripheral compartments, it rapidly antagonizes presynaptic α2 receptors on peripheral sympathetic terminals. Peripheral action does not require strong BBB penetration and is fully compatible with tolazoline's ADME properties. Sufficient central a2 antagonism is potentially aided by transporter dynamics and exposure timing. Despite a low BBB penetration probability for tolazoline, shared P-gp substrate status and xylazine's strong MRP1 inhibition can shift the efflux/entry balance so that enough tolazoline reaches the CNS quickly, especially given the very large free circulating pool ready to cross down a concentration gradient. Once there, competitive antagonism at α2 sites decreases the levels of sedation and analgesia, which is what is typically clinically observed.

Tolazoline is considered an appropriate antidote for xylazine intoxications in ruminants (Debnath and Chawla, 2023). It is routinely used in veterinary medicine at intravenous doses ranging from 1 to 4 mg/kg for the reversal of xylazine sedation and toxicity. Horses typically receive around 4 mg/kg IV, administered slowly to minimize cardiovascular side effects, while lower doses (1–2 mg/kg IV) are used for cattle and other animals (https://www.drugs.com/vet/tolazil.html). However, while veterinary doses could provide guidelines, clinical translation is limited by a lack of human data and differing pharmacodynamics, especially with co-exposure to opioids like fentanyl. For combined xylazine-fentanyl intoxication, experimental animal data are limited; tolazoline alone may not fully reverse the combined respiratory depression caused by both agents. An effective approach in animal models uses a combination of naloxone, for fentanyl, plus selective alpha-2 antagonists such as atipamezole, for xylazine (Yalakala et al., 2025). Probably, the naloxone plus atipamezole combination, could offer a safer and more effective approach than using a naloxone plus tolazoline combination, being tolazoline less selective, with an eventual higher rate and varied side effect profile (https://www.drugs.com/vet/tolazil.html). Finally, in our opinion, a direct comparison between atipamezole and tolazoline use in clinical trials would be beneficial, and we are actively working on the prediction of the atipamezole and similar molecules behavior in this context.

Although α2-adrenoceptors represent the primary pharmacological target for both compounds, we did not directly model these receptors. The BBB and transporter outputs are probabilistic and do not substitute for measured brain unbound concentrations. The mechanistic steps involving P-gp competition and MRP1 modulation are inferences based on the observed probabilities (P-gp substrate for both; strong MRP1 inhibition by xylazine; borderline MRP1 inhibition, by tolazoline). These steps are biologically plausible and consistent with observed clinical reversal, but confirmatory transporter-level experiments would be required. Receptor pharmacology, *per se* (e.g., α2-agonism for xylazine, α-antagonism for tolazoline), is not contained in the ADMET tables; the argument here is how ADME features facilitate or constrain those pharmacodynamic interactions *in vivo*. In summary, from an ADME perspective, xylazine is able to reach the central nervous system rapidly and to a significant extent, owing to its almost certain penetration of the blood-brain barrier, its moderate lipophilicity and its short half-life, which is nevertheless sufficient to induce a state of central action mediated by α2 receptors. Conversely, tolazoline, although less CNS-optimized, may compensate through exceptionally high unbound exposure, rapid compartment access, and a longer elimination half-life that outlasts the agonist. The two drugs' shared predicted P-gp substrate status and xylazine's predicted strong MRP1 inhibition create a transporter environment in which tolazoline can achieve enough central penetration quickly to competitively antagonize α2 receptors, while peripheral α-blockade promptly restores sympathetic tone. These predicted ADME profiles shed light on tolazoline's ability to reverse xylazine's effects *in vivo* and yield clear, testable predictions for transporter-aware PK/PD studies.

5 Conclusion

The current significant levels of xylazine identification in combination with misusing opiates/opioids have increased the perceived volatility within local drug markets, which has also undermined participants' confidence in the effectiveness of

naloxone (Sisson et al., 2025). Hence, there is a clinical need to implement appropriate treatment and management packages to counteract the acute toxicity associated with the combined use of mu- and α2-receptor agonists (Mullins and Seger, 2025). While other molecules could be considered as further potential candidates as counteracting agents (e.g., yohimbine, atipamezole, and prazosin), taken together, our findings support a mechanistic interpretation in which tolazoline's favorable kinetic and distributional properties, combined with its receptor competition profile, underpin its clinical efficacy in reversing xylazine intoxication. Finally, future studies should also investigate the risks posed by the recent emergence of metedomidine, whilst assessing the potential of tolazoline in reversing its effects as well.

Data availability statement

The original contributions presented in the study are included in the article/Supplementary Material, further inquiries can be directed to the corresponding author.

Author contributions

GF: Conceptualization, Writing – review and editing, Supervision, Resources, Project administration, Writing – original draft. VP: Visualization, Conceptualization, Formal Analysis, Writing – review and editing, Supervision, Writing – original draft. AG: Resources, Investigation, Writing – original draft, Validation, Methodology. DA: Methodology, Investigation, Writing – original draft, Validation. GP: Investigation, Writing – review and editing, Resources. AG: Investigation, Resources, Writing – review and editing. JMC: Writing – review and editing, Investigation, Resources. GM: Investigation, Resources, Writing – review and editing. SS: Writing – review and editing, Investigation, Resources. FS: Resources, Writing – review and editing, Validation, Investigation, Methodology.

Funding

The author(s) declared that financial support was not received for this work and/or its publication.

Conflict of interest

The author(s) declared that this work was conducted in the absence of any commercial or financial relationships that could be construed as a potential conflict of interest.

Generative AI statement

The author(s) declared that generative AI was used in the creation of this manuscript. In the preparation of this article, the authors made limited and transparent use of generative artificial intelligence (AI) tools to improve the clarity and consistency of text formulation, while ensuring full intellectual and scientific ownership of the content. Specifically, AI-assisted drafting tools (OpenAI ChatGPT and Grammarly) were employed exclusively for: • linguistic refinement (grammar, syntax, and terminology harmonisation); • generation of alternative phrasings to enhance readability. No AI tool was used to produce scientific, methodological, or strategic content.

Any alternative text (alt text) provided alongside figures in this article has been generated by Frontiers with the support of artificial intelligence and reasonable efforts have been made to ensure accuracy, including review by the authors wherever possible. If you identify any issues, please contact us.

Publisher's note

Supplementary material

The Supplementary Material for this article can be found online at: https://www.frontiersin.org/articles/10.3389/fchbi.2026.1806456/full#supplementary-material

References

Arena, E., Dichiara, M., Floresta, G., Parenti, C., Marrazzo, A., Pittalà, V., et al. (2018). Novel Sigma-1 receptor antagonists: from opioids to small molecules: what is new? *Future Medicinal Chemistry* 10 (2), 231–256. doi:10.4155/fmc-2017-0164

Azman, M., Sabri, A. H., Anjani, Q. K., Mustaffa, M. F., and Hamid, K. A. (2022). Intestinal absorption study: challenges and absorption enhancement strategies in improving oral drug delivery. *Pharm. (Basel)* 15 (8), 975. doi:10.3390/ph15080975

Bedard, M. L., Huang, X. P., Murray, J. G., Nowlan, A. C., Conley, S. Y., Mott, S. E., et al. (2024). Xylazine is an agonist at kappa opioid receptors and exhibits sex-specific responses to opioid antagonism. *Addict. Neurosci.* 11, 100155. doi:10.1016/j.addicn.2024.100155

Cano, M., Daniulaityte, R., and Marsiglia, F. (2024). Xylazine in overdose deaths and forensic drug reports in US states, 2019-2022. *JAMA Netw. Open* 7 (1), e2350630. doi:10.1001/jamanetworkopen.2023.50630

Casbeer, H. C., and Knych, H. K. (2013). Pharmacokinetics and pharmacodynamic effects of tolazoline following intravenous administration to horses. *Vet. J.* 196 (3), 504–509. doi:10.1016/j.tvjl.2012.12.006

Cheng, A., Best, S. A., Merz Jr, K. M., and Reynolds, C. H. (2000). GB/SA water model for the merck molecular force field (MMFF). *J. Mol. Graph. Model.* 18 (3), 273–282. doi:10.1016/s1093-3263(00)00038-3

Choi, S., Irwin, M. R., and Kiyatkin, E. A. (2023). Xylazine effects on opioid-induced brain hypoxia. *Psychopharmacol. Berl.* 240 (7), 1561–1571. doi:10.1007/s00213-023-06390-y

Choi, S., Irwin, M. R., Noya, M. R., Shaham, Y., and Kiyatkin, E. A. (2024). Combined treatment with naloxone and the alpha2 adrenoceptor antagonist atipamezole reversed brain hypoxia induced by a fentanyl-xylazine mixture in a rat model. *Neuropsychopharmacology* 49 (7), 1104–1112. doi:10.1038/s41386-023-01782-2

Choon, L. K., Khiruddin, A. I., Annuar, W., and Shamsuddin, S. R. (2023). A case series of accidental xylazine intoxication in humans; is there a role of naloxone as an antidote? *Turk J. Emerg. Med.* 23 (2), 119–122. doi:10.4103/tjem.tjem_198_22

Costanzo, G., Patamia, V., Turnaturi, R., Parenti, C., Zagni, C., Lombino, J., et al. (2023). Design, synthesis, *in vitro* evaluation, and molecular modeling studies of N-substituted benzomorphans, analogs of LP2, as novel MOR ligands. *Chem. Biol. Drug Des.* 101 (6), 1382–1392. doi:10.1111/cbdd.14220

Debnath, R., and Chawla, P. A. (2023). Xylazine addiction turning humans to zombies: fact or myth? *Health Sci. Rev.* 9, 100132. doi:10.1016/j.hsr.2023.100132

Demery, C., Moore, S. C., Levitt, E. S., Anand, J. P., and Traynor, J. R. (2025). Xylazine exacerbates fentanyl-induced respiratory depression and bradycardia. *J. Pharmacol. Exp. Ther.* 392 (7), 103616. doi:10.1016/j.jpet.2025.103616

Di Trana, A., Di Giorgi, A., Carlier, J., Serra, F., Busardò, F. P., and Pichini, S. (2024). Tranq-dope: the first fatal intoxication due to xylazine-adulterated heroin in Italy. *Clin. Chim. Acta* 561, 119826. doi:10.1016/j.cca.2024.119826

Dunn, J., Schifano, F., Dudley, E., and Guirguis, A. (2024). Exploring human misuse and abuse of veterinary drugs: a descriptive pharmacovigilance analysis utilising the food and drug administration's adverse events reporting system (FAERS). *Toxics* 12 (11), 777. doi:10.3390/toxics12110777

Fallica, A. N., Sorrenti, V., D'Amico, A. G., Salerno, L., Romeo, G., Intagliata, S., et al. (2021). Discovery of novel acetamide-based heme oxygenase-1 inhibitors with potent *in vitro* antiproliferative activity. *J. Med. Chem.* 64 (18), 13373–13393. doi:10.1021/acs.jmedchem.1c00633

Floresta, G., Pittala, V., Sorrenti, V., Romeo, G., Salerno, L., and Rescifina, A. (2018). Development of new HO-1 inhibitors by a thorough scaffold-hopping analysis. *Bioorg. Chem.* 81, 334–339. doi:10.1016/j.bioorg.2018.08.023

Floresta, G., Amata, E., Gentile, D., Romeo, G., Marrazzo, A., Pittalà, V., et al. (2019). Fourfold filtered statistical/computational approach for the identification of imidazole compounds as HO-1 inhibitors from natural products. *Mar. Drugs* 17 (2), 113. doi:10.3390/md17020113

Floresta, G., Patamia, V., Gentile, D., Molteni, F., Santamato, A., Rescifina, A., et al. (2020). Repurposing of FDA-Approved drugs for treating iatrogenic botulism: a paired 3D-QSAR/Docking approach. *ChemMedChem* 15 (2), 256–262. doi:10.1002/cmdc.201900594

Floresta, G., Granzotto, A., Patamia, V., Arillotta, D., Papanti, G. D., Guirguis, A., et al. (2025). Xylazine as an emerging new psychoactive substance; focuses on both 5-HT(7) and κ-opioid receptors' molecular interactions and isosteric replacement. *Arch. Pharm. Weinh.* 358 (3), e2500041. doi:10.1002/ardp.202500041

Friedman, J., Montero, F., Bourgois, P., Wahbi, R., Dye, D., Goodman-Meza, D., et al. (2022). Xylazine spreads across the US: a growing component of the increasingly synthetic and polysubstance overdose crisis. *Drug Alcohol Depend.* 233, 109380. doi:10.1016/j.drugalcdep.2022.109380

Fu, L., Shi, S., Yi, J., Wang, N., He, Y., Wu, Z., et al. (2024). ADMETlab 3.0: an updated comprehensive online ADMET prediction platform enhanced with broader coverage, improved performance, API functionality and decision support. *Nucleic Acids Research* 52 (W1), W422–W431. doi:10.1093/nar/gkae236

Garcia-Villar, R., Toutain, P. L., Alvinerie, M., and Ruckebusch, Y. (1981). The pharmacokinetics of xylazine hydrochloride: an interspecific study. *J. Vet. Pharmacol. Ther.* 4 (2), 87–92. doi:10.1111/j.1365-2885.1981.tb00715.x

Hagan, J. J., Price, G. W., Jeffrey, P., Deeks, N. J., Stean, T., Piper, D., et al. (2000). Characterization of SB-269970-A, a selective 5-HT(7) receptor antagonist. *Br. J. Pharmacol.* 130 (3), 539–548. doi:10.1038/sj.bjp.0703357

Hill, K., Heimer, R., and Sue, K. L. (2025). Everybody's liking it intentional use of xylazine in fentanyl among people Who use drugs. *Subst. Use Misuse* 61, 1–8. doi:10.1080/10826084.2025.2549499

Hoffman, G. R., Giduturi, C., Cordaro, N. J., Yoshida, C. T., Schoffstall, A. M., Stabio, M. E., et al. (2024). Classics in chemical neuroscience: xylazine. *ACS Chem. Neurosci.* 15 (11), 2091–2098. doi:10.1021/acschemneuro.4c00172

Hornak, V., Abel, R., Okur, A., Strockbine, B., Roitberg, A., and Simmerling, C. (2006). Comparison of multiple amber force fields and development of improved protein backbone parameters. *Proteins Struct. Funct. Bioinforma.* 65 (3), 712–725. doi:10.1002/prot.21123

Iacopetta, D., Catalano, A., Aiello, F., Andreu, I., Sinicropi, M. S., and Lentini, G. (2025). Xylazine, a drug adulterant whose use is spreading in the human population from the U.S. to the U.K. and all Europe: an updated review. *Appl. Sci.* 15 (6), 3410. doi:10.3390/app15063410

Ielo, L., Patamia, V., Citarella, A., Efferth, T., Shahhamzehei, N., Schirmeister, T., et al. (2022). Novel class of proteasome inhibitors: *in silico* and *in vitro* evaluation of diverse chloro(trifluoromethyl)aziridines. *Int. J. Mol. Sci.* 23 (20), 12363. doi:10.3390/ijms232012363

Jakalian, A., Jack, D. B., and Bayly, C. I. (2002). Fast, efficient generation of high-quality atomic charges. AM1-BCC model: II. Parameterization and validation. *J. Computational Chemistry* 23 (16), 1623–1641. doi:10.1002/jcc.10128

Kariisa, M., O'Donnell, J., Kumar, S., Mattson, C. L., and Goldberger, B. A. (2023). Illicitly manufactured fentanyl-involved overdose deaths with detected xylazine - united States, January 2019-June 2022. *MMWR Morb. Mortal. Wkly. Rep.* 72 (26), 721–727. doi:10.15585/mmwr.mm7226a4

Kelly, P. J. A., Green, T. C., Rich, J. D., Vento, S. A., Bailey, A., Silva, V., et al. (2025). Xylazine awareness and suspected presence in the illicit drug supply among people who used stimulants in an overdose hotspot, 2023. *Subst. Use Misuse* 61, 1–10. doi:10.1080/10826084.2025.2549501

Krieger, E., and Vriend, G. (2014). YASARA view - molecular graphics for all devices - from smartphones to workstations. *Bioinformatics* 30 (20), 2981–2982. doi:10.1093/bioinformatics/btu426

Krieger, E., Nielsen, J. E., Spronk, C. A., and Vriend, G. (2006). Fast empirical pKa prediction by Ewald summation. *J. Molecular Graphics Modelling* 25 (4), 481–486. doi:10.1016/j.jmgm.2006.02.009

Krieger, E., Dunbrack, R. L., Jr., Hooft, R. W., and Krieger, B. (2012). Assignment of protonation states in proteins and ligands: combining pKa prediction with hydrogen bonding network optimization. *Methods Mol. Biol.* 819, 405–421. doi:10.1007/978-1-61779-465-0_25

Kumar, A. H. (2024). Network pharmacology of xylazine to understand its health consequences and develop mechanistic based remediations. *bioRxiv* 2024 ,1–15. doi:10.1101/2024.02.08.579475

Kwon, H., Lionberger, R. A., and Yu, L. X. (2004). Impact of P-glycoprotein-mediated intestinal efflux kinetics on oral bioavailability of P-glycoprotein substrates. *Mol. Pharm.* 1 (6), 455–465. doi:10.1021/mp049921x

Maier, J. A., Martinez, C., Kasavajhala, K., Wickstrom, L., Hauser, K. E., and Simmerling, C. (2015). ff14SB: improving the accuracy of protein side chain and backbone parameters from ff99SB. *J. Chemical Theory Computation* 11 (8), 3696–3713. doi:10.1021/acs.jctc.5b00255

Mohammad, F. K., Mohammed, A. A., Rashid, H. M., and Garmavy, H. M. (2024). *In silico* identification of body proteins targeted by sedative analgesics xylazine, medetomidine and detomidine in relation to their antagonists. *Health Biotechnol. Biopharma (HBB)* 8 (2), 44–62. doi:10.22034/hbb.2024.16

Mullins, M. E., and Seger, D. L. (2025). Urgent need for reversal agents for xylazine and other imidazolines in illicit fentanyl. *Am. J. Emerg. Med.* 97, 129–130. doi:10.1016/j.ajem.2025.07.042

Nahid, N. A., and Johnson, J. A. (2022). CYP2D6 pharmacogenetics and phenoconversion in personalized medicine. *Expert Opin. Drug Metab. Toxicol.* 18 (11), 769–785. doi:10.1080/17425255.2022.2160317

Owusu-Antwi, P., Atodaria, P., Appiah-Kubi, E., Shah, Z., and Garcia, E. M. (2025). Management of xylazine toxicity, overdose, dependence, and withdrawal: a systematic review. *Am. J. Addict.* 34, 589–602. doi:10.1111/ajad.70051

Papudesi, B. N., Malayala, S. V., and Regina, A. C. (2023). *Xylazine toxicity*.

Patamia, V., Floresta, G., Zagni, C., Pistarà, V., Punzo, F., and Rescifina, A. (2023). 1,2-Dibenzoylhydrazine as a multi-inhibitor compound: a morphological and docking study. *Int. J. Mol. Sci.* 24 (2), 1425. doi:10.3390/ijms24021425

Pergolizzi, J., Jr., LeQuang, J. A. K., Magnusson, P., Miller, T. L., Breve, F., and Varrassi, G. (2023). The new stealth drug on the street: a narrative review of xylazine as a street drug. *Cureus* 15 (6), e40983. doi:10.7759/cureus.40983

Read, M. R., Duke, T., and Toews, A. R. (2000). Suspected tolazoline toxicosis in a llama. *J. Am. Vet. Med. Assoc.* 216 (2), 227–229. doi:10.2460/javma.2000.216.227

Rimawi, M., and Hamlin, D. (2025). *Xylazine: a review of intoxication, overdose, and withdrawal symptoms*. Washington, DC: American Psychiatric Association.

Santonastaso, A., Hardy, J., Cohen, N., and Fajt, V. (2014). Pharmacokinetics and pharmacodynamics of xylazine administered by the intravenous or intra-osseous route in adult horses. *J. Vet. Pharmacol. Ther.* 37 (6), 565–570. doi:10.1111/jvp.12136

Schifano, F., Orsolini, L., Duccio Papanti, G., and Corkery, J. M. (2015). Novel psychoactive substances of interest for psychiatry. *World Psychiatry* 14 (1), 15–26. doi:10.1002/wps.20174

Schifano, F., Orsolini, L., Papanti, D., and Corkery, J. (2017). NPS: medical consequences associated with their intake. *Curr. Top. Behav. Neurosci.* 32, 351–380. doi:10.1007/7854_2016_15

Shafi, A., Berry, A. J., Sumnall, H., Wood, D. M., and Tracy, D. K. (2020). New psychoactive substances: a review and updates. *Ther. Adv. Psychopharmacol.* 10, 2045125320967197. doi:10.1177/2045125320967197

Sibley, A. L., Bedard, M. L., Tobias, S., Chidgey, B. A., Phillips, I. G., Bell, A., et al. (2025). Emergence of medetomidine in the unregulated drug supply and its association with hallucinogenic effects. *Drug Alcohol Rev.* 44, 1896–1906. doi:10.1111/dar.70024

Sisson, L. N., Winiker, A. K., Triece, T., Rousch, R. S., Rouhani, S., Owczarzak, J., et al. (2025). All you can Do is what you know to do: naloxone knowledge and uncertainty among people who use drugs in Maryland amid a volatile drug market. *Subst. Use Misuse* 60 (8), 1164–1172. doi:10.1080/10826084.2025.2491768

Smith, M. A., Biancorosso, S. L., Camp, J. D., Hailu, S. H., Johansen, A. N., Morris, M. H., et al. (2023). "Tranq-dope" overdose and mortality: lethality induced by fentanyl and xylazine. *Front. Pharmacology* 14, 1280289. doi:10.3389/fphar.2023.1280289

Smith, M. A., Spera, A. G., Thomas, E. M., Biancorosso, S. L., and Carlson, H. N. (2025). Mu-opioid mediated discriminative stimulus effects of fentanyl and xylazine: dose-response and time-course studies. *Drug Alcohol Depend.* 275, 112799. doi:10.1016/j.drugalcdep.2025.112799

Stewart, J. J. (2004). Optimization of parameters for semiempirical methods IV: extension of MNDO, AM1, and PM3 to more main group elements. *J. Mol. Model.* 10 (2), 155–164. doi:10.1007/s00894-004-0183-z

Stoeckelhuber, B. M., Suttmann, I., Stoeckelhuber, M., and Kueffer, G. (2003). Comparison of the vasodilating effect of nitroglycerin, verapamil, and tolazoline in hand angiography. *J. Vasc. Interv. Radiol.* 14 (6), 749–754. doi:10.1097/01.rvi.0000079984.80153.5e

Wang, J., Wolf, R. M., Caldwell, J. W., Kollman, P. A., and Case, D. A. (2004). Development and testing of a general amber force field. *J. Computational Chemistry* 25 (9), 1157–1174. doi:10.1002/jcc.20035

Yalakala, J., Tackett, W. R., Varney, M. E., Davies, T. H., and Hambuchen, M. D. (2025). Co-administration of naloxone and atipamezole to simultaneously reverse the acute effects of fentanyl and xylazine in rats. *J. Transl. Res.* 2 (1), 2493044. doi:10.1080/29947448.2025.2493044

Yi, S., Mai, T., Fang, Y., Tian, Q., and Zhao, S. (2025). Repeated injection of xylazine causes liver injury through the PPAR signaling pathway in rats. *J. Biochem. Mol. Toxicol.* 39 (1), e70101. doi:10.1002/jbt.70101

Yu, Z., Yuan, Y., Zhang, J., Gao, X., Chen, C., Zhao, E., et al. (2025). Forensic pathology and toxicological analyses: a case of fatal xylazine poisoning. *J. Forensic Sci.* 70 (5), 2102–2107. doi:10.1111/1556-4029.70104

Zhu, D. T., Mitragotri, S., and Cano, M. (2025). Temporal and spatial patterns of xylazine and medetomidine detected in the DEA's national forensic laboratory information system (NFLIS) reports. *Soc. Sci. and Med.* 384, 118521. doi:10.1016/j.socscimed.2025.118521